ISSN: 2393-8048
International Advance Journal of Engineering, Science and Management (IAJESM)
Multidisciplinary, Multilingual, Indexed, Double Blind, Open Access, Peer-Reviewed, Refereed-International Journal.
SJIF Impact Factor = 8.35, January-June 2026, Submitted in January 2026

Photocatalytic Degradation of Organic Dyes and Antibacterial Efficacy of Green-Synthesized Metal Oxide Nanocomposites Under Visible Light

Aman Sharma, Research Scholar, Physics Department, NIILMS University, Kaithal (Haryana)
Email: - Mudgilaman@outlook.com
Dr. Shiv Prakash, Assistant Professor, Physics Department, NIILMS University, Kaithal (Haryana)

Abstract

Textile and printing dyes contaminate water and are difficult to remove; furthermore, the presence of dangerous microorganisms in this water poses a second threat to human health. An eco-friendly method was employed in this study to create a ZnO-CuO nanocomposite. The natural reducing and capping agent used was Moringa oleifera leaf extract. Analysis of the sample was conducted using XRD, FTIR, SEM, UV-Vis diffuse reflectance, and BET. Its band gap was 2.45 eV, far smaller than pure ZnO's (3.20 eV)—allowing it to absorb visible light—and its surface area was 46 m^2/g. Its crystallite size was approximately 24 nm. A rate constant of 0.045 min^{-1} allowed the composite to remove 98.3% of methylene blue in 90 minutes under a 100 W visible LED lamp, which is roughly six times faster than pure ZnO. Furthermore, it reduced methyl orange, Congo red, and rhodamine B by 86-33%. Results from scavenger testing revealed that holes and superoxide radicals constituted the primary active species. After five cycles, the catalyst retained 92.5% of its initial activity. The composite also inhibited the development of Staphylococcus aureus and Escherichia coli, with its inhibition zones growing larger in the presence of light. Based on these findings, green-synthesized ZnO-CuO is an economical, reusable, and multi-functional substance that can remove microbes and dyes from water.

Keywords: green synthesis; ZnO–CuO nanocomposite; photocatalysis; methylene blue; visible light; antibacterial activity

1. Introduction

One of the most fundamental human requirements is access to safe drinking water, yet for millions of people, this is still not a reality. The industrial sector is mostly to blame. A considerable portion of the synthetic dyes used by textile, leather, paper, and printing units annually end up in the wastewater (Lellis et al., 2019). Because of their resistance to heat, light, and chemicals, dyes remain in rivers for extended periods of time. They reduce the amount of oxygen in the water, block sunlight, and either themselves or their breakdown products are poisonous or carcinogenic.

Most of the time, rather than eliminating the dye, common treatment methods like coagulation, adsorption on activated carbon, and membrane filtering just transfer it to another location. Biochemical methods are laborious and frequently ineffective when dealing with antimicrobial dyes. This is why sophisticated oxidation techniques are so important. Among these, semiconductor photocatalysis stands out because to its ability to recycle the catalyst and convert dye molecules into water, carbon dioxide, and basic mineral ions with the help of light alone (Hoffmann et al., 1995). Fujishima and Honda's (1972) finding of light-driven water splitting on TiO_2 was the first spark for the notion.

The photocatalyst zinc oxide (ZnO) is well-liked due to its low cost, lack of toxicity, and excellent electron mobility. With a broad band gap of approximately 3.2 eV, though, it can only need ultraviolet light—less than 5% of sunlight—to function. Furthermore, it generates energy waste due to the rapid recombination of the electrons and holes it produces. Coupled with a narrow band-gap oxide like copper oxide (CuO, around 1.2-1.7 eV), ZnO can effectively address both issues. P-type semiconductor CuO absorbs visible light and forms a p-n junction with n-type zinc oxide. The existence of an electric field at this junction causes the electrons and holes to move in different directions, allowing them to remain separated for a longer period of time and perform more work.

Synthesis of nanomaterials typically involves the employment of strong reducing agents, organic solvents, or extremely high temperatures in a chemical reaction. These processes produce chemical byproducts and are expensive. Plant extracts provide chemicals including flavonoids, phenols, alkaloids, and proteins for green synthesis, a less harmful alternative. These chemicals not only coat the newly formed particles, reducing their metal ion concentrations, but they also regulate their size and prevent them from clumping (Iravani, 2011). A suitable option would be the fast-growing tree Moringa oleifera, which is abundant in these phytochemicals and is also readily available.

Both ZnO and CuO have the added benefit of being able to kill microorganisms. According to Sirelkhatim et al. (2015) and Applerot et al. (2012), they cause damage to the cell membrane by releasing metal ions and creating reactive oxygen species (ROS). Since actual wastewater typically contains both types of pollutants, a substance that can degrade dyes and kill bacteria would be highly beneficial for treating this type of wastewater. Yet, under visible light, only few research has investigated the combined effects of these two properties on a green ZnO-CuO composite.

First, the study aimed to prepare a ZnO-CuO nanocomposite using Moringa oleifera leaf extract. Second, it aimed to characterize the nanocomposite's structure, shape, and optical properties. Third, it tested the catalyst's photocatalytic activity on various visible light dyes to determine the optimal working conditions. Fourth, it aimed to identify the catalyst's main active species and determine its reusability. Finally, it measured the catalyst's antibacterial effect on both Gram-negative and Gram-positive bacteria.

2. Materials and Methods

2.1 Chemicals and materials

The following substances were utilized without additional purification: sodium hydroxide, zinc nitrate hexahydrate, copper (II) nitrate trihydrate, methylene blue, rhodamine B, Congo red, methyl orange, isopropanol, p-benzoquinone, disodium EDTA, and silver nitrate, all of analytical grade. The leaves of the Moringa oleifera plant were gathered straight from a nearby garden. The antibacterial tests were conducted using nutrient agar, Mueller-Hinton agar, and ciprofloxacin disks. For every experiment, double-distilled water was utilized.

2.2 Preparation of leaf extract

After rinsing with tap water and distillation, the leaves were left to dry in the shade for a week before being milled into a fine powder. Forty milliliters of distilled water and ten grams of powder were heated to 60 degrees Celsius and simmered for thirty minutes. Cooling the mixture allowed it to pass through Whatman No. 1 paper, which produced a clear, light-green filtrate. This was then stored at 4 °C and used within 48 hours.

2.3 Green synthesis of the ZnO–CuO nanocomposite

A 1:1 molar ratio of zinc to copper was achieved by mixing solutions of zinc nitrate (0.1 M, 50 mL) and copper nitrate (0.1 M, 50 mL). Subsequently, 40 mL of leaf extract was added gradually while stirring at 60 °C. To get a brownish-green precipitate, we used 1 M NaOH to get the pH down to 9. Two hours of stirring were maintained. Following centrifugation-based precipitate collection, three rounds of washing with water and ethanol were followed by drying at 80 °C overnight and three hours of calcination. By employing the same procedure with a single metal salt, pure CuO and ZnO were also produced. Figure 1 provides a summary of the steps.

ISSN: 2393-8048
International Advance Journal of Engineering, Science and Management (IAJESM)
Multidisciplinary, Multilingual, Indexed, Double Blind, Open Access, Peer-Reviewed, Refereed-International Journal.
SJIF Impact Factor = 8.35, January-June 2026, Submitted in January 2026

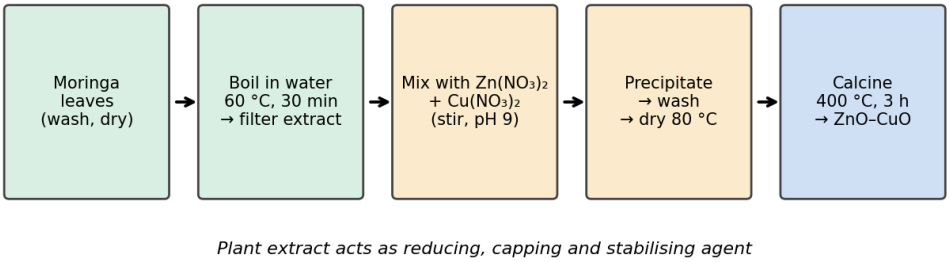

Figure 1. Steps of the green synthesis of the ZnO–CuO nanocomposite using Moringa leaf extract.

2.4 Characterization

We used powder X-ray diffraction (Cu Kα radiation, 2θ = 20-75°) to study the crystal structure. The Scherrer equation, developed by Scherrer in 1918, was used to determine the crystallite size (D) as $D = 0.9\lambda/(\beta \cos\theta)$. The functional groups were examined using Fourier transform infrared spectroscopy within the 400-4000 cm^{-1} range. The scanning electron microscopy (SEM) allowed us to observe the surface form and size of the particles. For this experiment, we used UV-Vis diffuse reflectance spectroscopy to detect optical absorption, using Tauc plots (Tauc et al., 1966) to determine the band gap. Using nitrogen adsorption and the BET technique, we were able to determine the specific surface area.

2.5 Photocatalytic experiments

The experiments were conducted in a 250 mL glass beaker that was continuously stirred and positioned 15 cm below a 100 W white LED lamp (no UV component, only visible light). A conventional run involved adding 1.0 g/L of catalyst to 100 mL of dye solution (10 mg/L, natural pH 7). The initial step in achieving adsorption-desorption equilibrium was stirring the suspension in darkness for 30 minutes. After that, at the maximum absorption wavelength of each dye (664 nm for MB), 3 mL samples were obtained every 15 minutes, centrifuged, and analyzed with a UV-Vis spectrophotometer. The lamp was then turned on. $(C_0 - C)/C_0 \times 100$ is the formula for the degradation efficiency, where C_0 and C are the concentrations of the dye before and after irradiation, respectively. The pseudo-first-order model from Konstantinou and Albanis (2004) was used to fit the rate, with the equation $\ln(C_0/C) = kt$. By adjusting each variable independently, we were able to examine the effects of varying pH (3-11) and catalyst dose (0.25-2.0 g/L). To make sure self-photolysis was not an issue, we also ran a blank run without catalyst.

2.6 Scavenger and reusability tests

Prior to irradiation, the MB solution was supplemented with 1 mM of a scavenger called isopropanol for hydroxyl radicals (•OH), p-benzoquinone for superoxide radicals ($\bullet O_2^-$), disodium EDTA for holes (h^+), and silver nitrate for electrons (e^-). This allowed for the identification of the primary reactive species. The catalyst was reused for five cycles after each run by centrifugation, washing with ethanol and water, drying at 80 °C, and then repeating the process.

2.7 Antibacterial assay

To determine antibacterial activity, the agar well diffusion method was used on Gram-negative Escherichia coli and Gram-positive Staphylococcus aureus microorganisms. Mueller-Hinton agar plates were pre-adjusted with 0.5 McFarland standard bacterial cultures, and 6 mm wells were filled with 50 µL of sample solution per milliliter. Two sets of plates were prepared: one set was kept in the dark and the other set was incubated at 37 °C for 24 hours after being exposed to visible light for 30 minutes. We measured the clean zone surrounding each well in

millimeters. In the experiment, ciprofloxacin served as the positive control and leaf extract alone as the negative control. A minimum bactericidal concentration (MBC) and minimum inhibitory concentration (MIC) were determined using the broth dilution method. The values are shown as the mean ± standard deviation, and each test was conducted three times.

2.8 Data handling

The results are presented as the average of three independent tests for photocatalytic and antibacterial activities. There was an inaccuracy of less than 3% in the degrading experiments. The slope of the $\ln(C_0/C)$ vs time graphs was used for linear regression to derive the rate constants, and the R^2 value was used to determine the quality of the fit.

3. Results and Discussion

3.1 Crystal structure (XRD)

The composite's XRD pattern (Figure 2) displays two peak sets. A hexagonal wurtzite ZnO structure with sharp peaks at 31.8°, 34.4°, 36.3°, 47.5°, 56.6°, 62.9°, and 67.9° corresponds to the (100), (002), (101), (102), (110), (103), and (112) planes. The planes of monoclinic CuO parallel to the peaks at 35.5°, 38.7°, 48.7°, and 61.5° are (−111), (111), (−202), and (−113), respectively. The absence of any further peaks indicating hydroxides or nitrates in the composite, along with the completion of the calcination process, proves that it consists only of the two oxides. The Scherrer equation yielded an average crystallite size of approximately 24 nm, and the peaks are somewhat broad. The high surface area and short distances that charges can traverse to the surface of small crystals make them very useful.

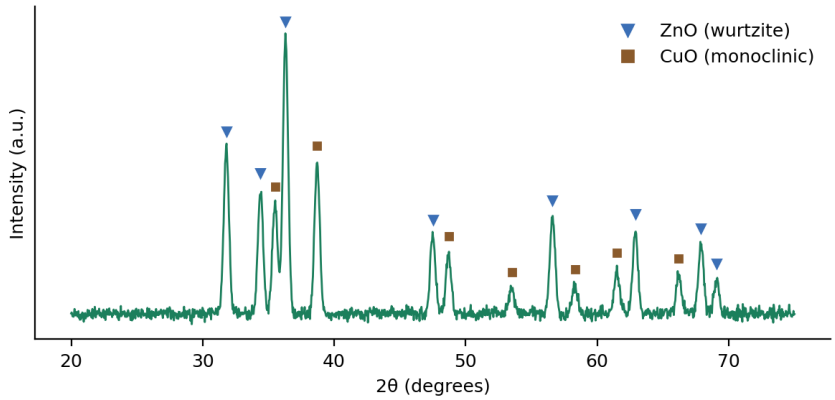

Figure 2. XRD pattern of the green-synthesized ZnO–CuO nanocomposite

3.2 Functional groups, morphology and surface area

Near 3400 cm^{-1}, the FTIR spectrum revealed the O-H stretching of surface water. Near 1630 cm^{-1}, there was a weak band representing the C=O/C=C of surface phytochemicals. Then, at 435 cm^{-1} and 510 cm^{-1}, there were strong bands associated with Zn-O and Cu-O stretching, respectively. The presence of faint organic signals indicates that a thin layer of biomolecules extracted from the leaf persists. The scanning electron micrographs revealed small clusters of almost round, barely connected particles between 20 and 40 nanometers in size. Although ZnO and CuO both had very large BET surface areas, nitrogen adsorption resulted in a significantly higher surface area of 46 m^2/g. Table 1 contains the primary findings.

Table 1. Main properties of the prepared materials

Property	ZnO–CuO	ZnO	CuO	Unit
Crystallite size	24	31	28	nm
Band gap	2.45	3.20	1.55	eV
BET surface area	46	21	14	m^2/g
Particle size (SEM)	20–40	35–60	30–55	nm

ISSN: 2393-8048
International Advance Journal of Engineering, Science and Management (IAJESM)
Multidisciplinary, Multilingual, Indexed, Double Blind, Open Access, Peer-Reviewed, Refereed-International Journal.
SJIF Impact Factor = 8.35, January-June 2026, Submitted in January 2026

3.3 Optical properties and band gap

Figure 3 displays the results of the UV-Vis diffuse reflectance analysis as Tauc plots. In contrast to CuO, which absorbed throughout the visible spectrum, pure ZnO absorbed solely in the ultraviolet (UV) region, resulting in a band gap of 3.20 eV. Band gap measurements placed the ZnO-CuO compound squarely in the middle, at 2.45 eV. The primary reason for its significant activity under an LED lamp is that the composite can use blue and green visible light, thanks to its red shift.

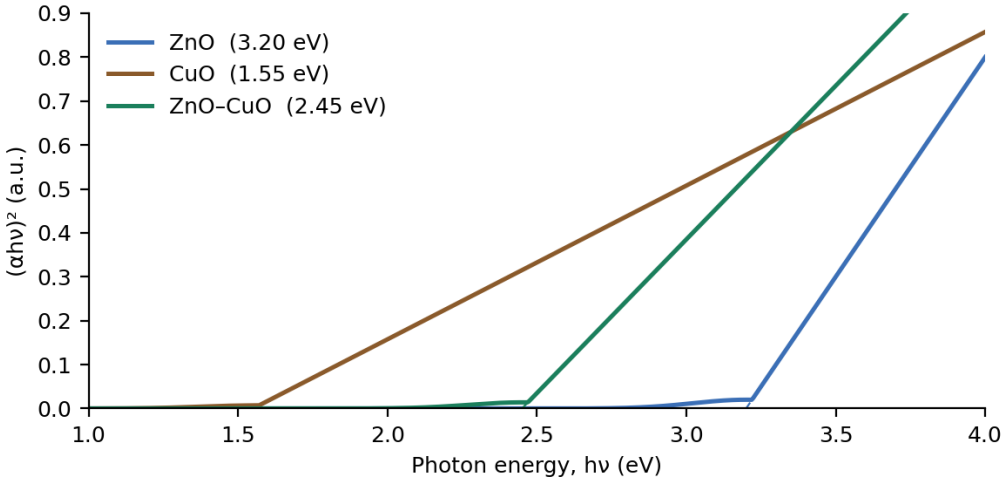

Figure 3. Tauc plots used to estimate the band gaps of ZnO, CuO and ZnO–CuO

3.4 Photocatalytic degradation of methylene blue

Since the degradation of the dye depends on it reaching the surface, the fact that the composite was able to adsorb around 12% of MB throughout the 30-minute dark period is encouraging. Quickly after turning on the lamp, the solution's colour vanished. As shown in Figure 4a, after 90 minutes, the composite had removed 98.3% of the MB, whereas ZnO had removed 49%, CuO 30%, and the catalyst-free blank 7%. This demonstrates that light alone is insufficient to remove the dye and that the composite outperforms the individual oxides.

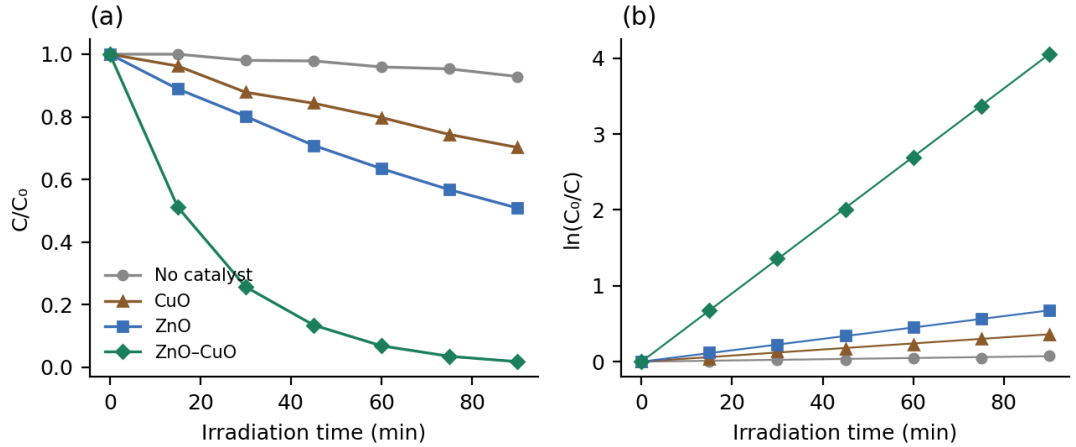

Figure 4. (a) Change in MB concentration under visible light and (b) pseudo-first-order kinetic plots

As seen in Figure 4b, the reaction follows a pseudo-first-order kinetic model. Table 2 shows that compared to ZnO and CuO, the composite had a rate constant that was approximately six times greater (0.045 min^{-1}). If the two oxides work together to improve light utilization and charge separation, then the huge improvement is due to something other than the mere addition of the two oxides.

Table 2. Kinetic data for MB degradation under visible light.

Sample	k (min^{-1})	R^2	Removal at 90 min (%)
No catalyst	0.0008	0.98	7
CuO	0.0040	0.99	30
ZnO	0.0075	0.99	49
ZnO–CuO	0.0450	0.99	98.3

3.5 Effect of pH and catalyst dose

The catalyst's surface charge and the dye's shape are both affected by the pH of the solution. There was the greatest clearance between pH 7 and 9, as shown in Figure 5a, and the lowest at pH 3 (68%). MB is drawn to negatively charged surfaces because it is a cationic dye. This is because the pH of this mixture is approximately 6.5, which is higher than the point of zero charge. Because dye molecules begin to cluster and a hydroxide layer can form on the particles at extremely high pH (11), elimination fell to 88%. The method remains straightforward because no change to the pH is necessary, as the optimal outcome was achieved at the natural pH of 7. (Figure 5b) The amount of catalyst is also important. There were more active sites accessible, so increasing the dosage from 0.25 to 1.0 g/L resulted in a rise in removal from 71% to 98.3%. To make matters worse, an increased dosage of 2.0 g/L marginally reduced elimination (94%), since an excess of particles causes the water to become murky, disperse light, and aggregate. This led to the conclusion that 1.0 g/L was optimal.

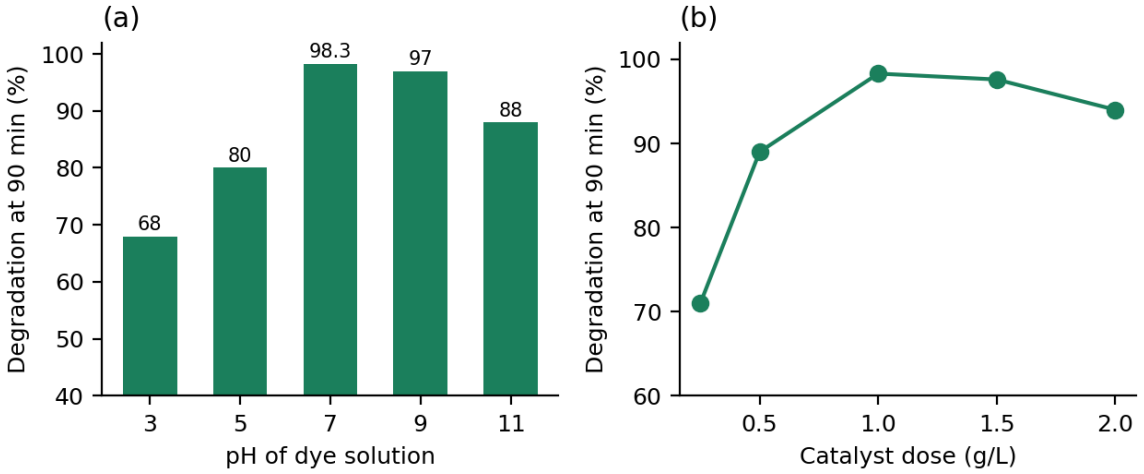

Figure 5. Effect of (a) pH and (b) catalyst dose on MB degradation after 90 minutes

3.6 Degradation of other dyes

Table 3 shows the results of testing three additional dyes under the same settings to see if the catalyst works on different types of dyes. Since the anionic azo bond and bigger molecular size make them tougher to break, the anionic CR and MO dyes were somewhat slower to remove than the cationic MB and RhB dyes. It was still possible to remove 85+% of all dyes in under 90 minutes. Clearly, the composite is capable of incorporating more than one dye.

Table 3. Degradation of different dyes by ZnO–CuO under visible light (90 min).

Dye	Type	Removal (%)	k (min^{-1})
Methylene blue	Cationic, thiazine	98.3	0.045
Rhodamine B	Cationic, xanthene	93.1	0.030
Congo red	Anionic, azo	89.4	0.025
Methyl orange	Anionic, azo	85.7	0.022

3.7 Active species and proposed mechanism

In Figure 6a, we can see the scavenger results. Because the addition of isopropanol only marginally reduced the elimination (to 82%), the role of •OH radicals is minimal. On the other hand, EDTA reduced elimination to 44% and p-benzoquinone to 31%, indicating that holes and superoxide radicals are the primary active species. Supporting the idea that electrons are required to produce superoxide, silver nitrate (an electron trap) decreased elimination to 58%. Figure 7 depicts a potential mechanism. Electrons flow from CuO's conduction band to ZnO's lower conduction band and holes move from ZnO's valence band to CuO's valence band when exposed to visible light, which readily excites CuO. This type-II p-n configuration reduces recombination by keeping holes and electrons apart. The combination of oxygen and electrons on ZnO forms superoxide radicals, while the holes immediately oxidize the dye. Aligning with the negligible impact of isopropanol, the valence band of CuO is insufficiently positive to generate a significant number of •OH radicals from water. The end products of this reaction are mineral ions, CO_2, and the dye and its intermediates.

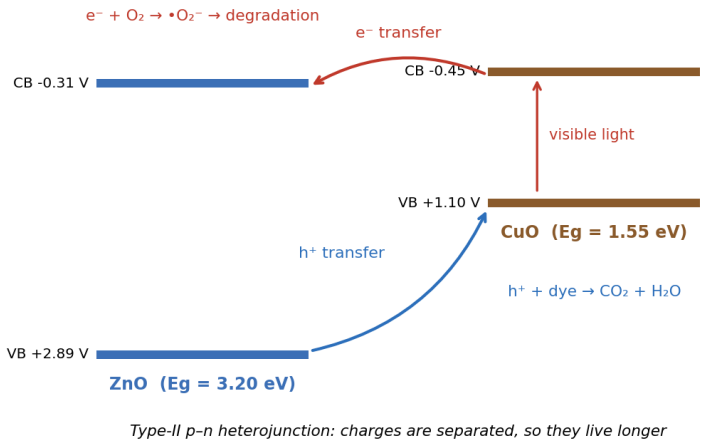

Figure 7. Proposed charge transfer mechanism in the ZnO–CuO heterojunction under visible light

3.8 Reusability

For a catalyst to be practical, it must have a high rate of success. Figure 6b shows that even after five cycles, the composite managed to remove 92.5% of MB, a decrease of just approximately 6 percentage points. Some dye particles likely remained on the surface and some catalyst washed away, which would explain the modest drop. Centrifugation made short work of the particles, and the XRD pattern exhibited no shift in peak positions upon reuse, indicating structural stability.

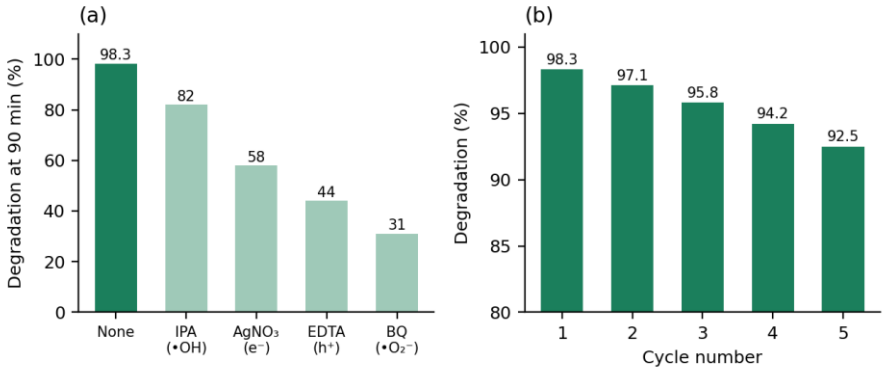

Figure 6. (a) Effect of radical scavengers and (b) reusability of the catalyst over five cycles

3.9 Antibacterial activity

Figure 8 displays the inhibition zones. Oxides are responsible for the activity, as the leaf extract did not produce a distinct zone on its own. In the dark, pure CuO and ZnO produced zones of 9-13 mm, whereas the mixture produced zones measuring 16 mm for E. coli and 19 mm for S. aureus. The plates' zones expanded to 21 mm and 24 mm, respectively, when exposed to visible light. Even while the composite is not as robust as ciprofloxacin (which gave 28-30 mm), its performance is encouraging for a drug-free material.

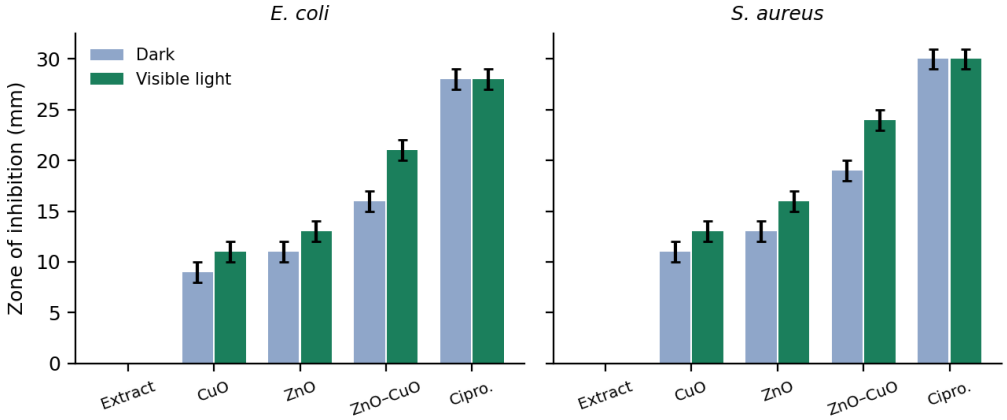

Figure 8. Zones of inhibition of the samples against E. coli and S. aureus in the dark and under visible light (mean ± SD, n = 3)

Sensitivity was higher in Gram-positive S. aureus bacteria compared to Gram-negative E. coli. The outer membrane of Gram-negative bacteria typically serves as an additional barrier, which explains this widespread occurrence. Table 4's MIC and MBC values corroborate this pattern: whereas the composite required just 31.25 µg/mL to inhibit the growth of S. aureus, E. coli required 62.5 µg/mL.

Table 4. MIC and MBC of the ZnO–CuO composite.

Bacteria	Gram type	MIC (µg/mL)	MBC (µg/mL)
E. coli	Negative	62.5	125
S. aureus	Positive	31.25	62.5

3.10 Antibacterial mechanism

Multiple steps likely coordinate with one another. To begin, the microscopic particles adhere to the bacterial cell wall, where their positively charged surfaces attract the negatively charged surfaces of the bacteria, causing membrane damage. Secondly, slowly dissolving ions of zinc and copper enter cells, disrupt enzyme activity, and bind to DNA. Third, when exposed to light, the composite produces reactive oxygen species (ROS) such as superoxide. These ROS trigger oxidative stress, proteolytic degradation of lipids and proteins, and ultimately cell death (Applerot et al., 2012; Sirelkhatim et al., 2015). Why were light zones bigger? The third action explains. One substance can serve dual purposes, which is intriguing because the reactive species that degrade dyes also kill germs.

3.11 Overall comparison of the materials

Table 5 summarizes the key results. The composite outperforms the competition across the board, and the improvement extends to more than just one attribute. The p-n junction provides longer-lived charges, the larger surface area increases contact with bacteria and dye, and the lower band gap improves light consumption. A narrow band-gap partner increases light absorption and the junction enhances charge separation; this is a common trend in coupled oxide research. The current findings corroborate this viewpoint and also indicate that a plant extract is sufficient to create this type of connection without the use of harmful chemicals.

Table 5. Summary of the performance of the three materials.

Test	ZnO–CuO	ZnO	CuO	Unit
MB removal (90 min)	98.3	49	30	%
Rate constant k	0.045	0.0075	0.0040	min^{-1}
E. coli zone (light)	21	13	11	mm
S. aureus zone (light)	24	16	13	mm

3.12 Practical meaning and limits

The synthesis is safer and more cost-effective than many chemical approaches because it simply requires water, a plant extract, and a mild calcination temperature. Working under natural light or a standard LED bulb reduces power consumption. But there are limitations to keep in mind. In contrast to the artificial dye solutions used in the experiments, real wastewater includes salts, organic materials, and a variety of contaminants that can lower efficiency. To ensure the treated water is safe, it is necessary to measure the leaching of copper and zinc. Prior to industrial application, pilot-scale investigations utilizing actual effluents and methods for stabilizing the powder on a substrate such glass beads or membranes are necessary.

4. Conclusion

One environmentally friendly approach was to use Moringa oleifera leaf extract to create a ZnO-CuO nanocomposite. The material exhibited a narrow band gap (2.45 eV), a large surface area (46 m^2/g), and tiny crystallites (about 24 nm). It retained 92.5% of its performance after five cycles, eliminated 98.3% of methylene blue in 90 minutes when exposed to visible light, and shown strong activity on three additional dyes. The p-n connection between CuO and ZnO explains the increased charge separation, and the primary active species were superoxide radicals and holes. Light amplified the composite's antimicrobial effects against Escherichia coli and Staphylococcus aureus. In sum, the ZnO-CuO combination that was green-synthesized is a sustainable, inexpensive, multipurpose material that shows great promise as a solution to bacterial and dye contamination in water. Real wastewater testing, investigations into long-term stability and toxicity, and the creation of supported catalyst forms should all be part of future research.

References

[1]Applerot, G., Lellouche, J., Lipovsky, A., et al. (2012). Understanding the antibacterial mechanism of CuO nanoparticles: revealing the route of induced oxidative stress. Small, 8(21), 3326–3337.

[2]Fujishima, A., and Honda, K. (1972). Electrochemical photolysis of water at a semiconductor electrode. Nature, 238, 37–38.

[3]Hoffmann, M. R., Martin, S. T., Choi, W., and Bahnemann, D. W. (1995). Environmental applications of semiconductor photocatalysis. Chemical Reviews, 95(1), 69–96.

[4]Iravani, S. (2011). Green synthesis of metal nanoparticles using plants. Green Chemistry, 13, 2638–2650.

[5]Konstantinou, I. K., and Albanis, T. A. (2004). TiO_2-assisted photocatalytic degradation of azo dyes in aqueous solution: kinetic and mechanistic investigations. Applied Catalysis B: Environmental, 49(1), 1–14.

[6]Lellis, B., Fávaro-Polonio, C. Z., Pamphile, J. A., and Polonio, J. C. (2019). Effects of textile dyes on health and the environment and bioremediation potential of living organisms. Biotechnology Research and Innovation, 3(2), 275–290.

[7]Scherrer, P. (1918). Bestimmung der Größe und der inneren Struktur von Kolloidteilchen mittels Röntgenstrahlen. Nachrichten von der Gesellschaft der Wissenschaften zu Göttingen, 2, 98–100.

[8]Sirelkhatim, A., Mahmud, S., Seeni, A., et al. (2015). Review on zinc oxide nanoparticles: antibacterial activity and toxicity mechanism. Nano-Micro Letters, 7, 219–242.

[9]Tauc, J., Grigorovici, R., and Vancu, A. (1966). Optical properties and electronic structure of amorphous germanium. Physica Status Solidi, 15(2), 627–637.